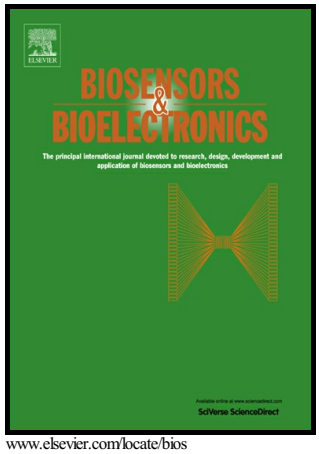

www.elsevier.com/locate/bios

A flexible and highly sensitive nonenzymatic glucose sensor based on DVD-laser scribed graphene substrate

Songyue Lin, Wendou Feng, Xiaofei Miao, Xiangxin Zhang, Sujing Chen, Yuanqiang Chen, Wei Wang, Yining Zhang

PII: S0956-5663(18)30195-7
DOI: https://doi.org/10.1016/j.bios.2018.03.019
Reference: BIOS10345

To appear in: *Biosensors and Bioelectronic*

Received date: 27 December 2017
Revised date: 1 March 2018
Accepted date: 12 March 2018

Cite this article as: Songyue Lin, Wendou Feng, Xiaofei Miao, Xiangxin Zhang, Sujing Chen, Yuanqiang Chen, Wei Wang and Yining Zhang, A flexible and highly sensitive nonenzymatic glucose sensor based on DVD-laser scribed graphene substrate, *Biosensors and Bioelectronic,* https://doi.org/10.1016/j.bios.2018.03.019

A flexible and highly sensitive nonenzymatic glucose sensor based on DVD-laser scribed graphene substrate

Songyue Lin[a, b], Wendou Feng[a, b], Xiaofei Miao[a], Xiangxin Zhang[a], Sujing Chen[a], Yuanqiang Chen[a], Wei Wang[a, b]*, Yining Zhang[a, b]*

[a] Key Laboratory of Optoelectronic Materials Chemistry and Physics, Fujian Institute of Research on the Structure of Matter, Chinese Academy of Sciences, 155 Yangqiao Road West, Fuzhou, Fujian 350002, P. R. China.

[b] University of Chinese Academy of Sciences, Beijing 100049, P. R. China

* *To whom correspondence should be addressed: wangwei@fjirsm.ac.cn and ynzhang@fjirsm.ac.cn.*

ABSTRACT

Flexible and implantable glucose biosensors are emerging technologies for continuous monitoring of blood-glucose of diabetes. Developing a flexible conductive substrates with high active surface area is critical for advancing the technology. Here, we successfully fabricate a flexible and highly sensitive nonenzymatic glucose by using DVD-laser scribed graphene (LSG) as a flexible conductively substrate. Copper nanoparticles (Cu-NPs) are electrodeposited as the catalyst. The LSG/Cu-NPs sensor demonstrates excellent catalytic activity toward glucose oxidation and exhibits a linear glucose detection range from 1 μM to 4.54 mM with high sensitivity (1.518 mA mM^{-1} cm^{-2}) and low limit of detection (0.35 μM). Moreover, the LSG/Cu-NPs sensor shows excellent reproducibility and long-term stability. It is also highly selective toward glucose oxidation under the presence of various interfering species. Excellent flexing stability is also demonstrated by the LSG/Cu-NPs sensor, which is capable of maintaining 83.9% of its initial current after being bent against a 4-mm diameter rod for 180 times. The LSG/Cu-NPs sensor shows great potential for practical application as a nonenzymatic glucose biosensor. Meanwhile, the LSG conductive substrate provides a platform for the developing next-generation flexible and potentially implantable bioelectronics and biosensors.

Keywords:
Laser-scribed graphene; Copper nanoparticles; Electrodeposition; Flexible conductive substrates; Glucose sensor; Flexible biosensors

1. Introduction

Millions of diabetics measure their blood-glucose levels on a daily basis. With more than 380 million people suffering from diabetes worldwide (Shi and Hu 2014), glucose sensor becomes one of the most important biological sensors. It is estimated that the glucose biosensor accounts for about 85% of the multi-billion biosensor market (Wang 2008). The huge market size and significant financial benefits have attracted great research interests into developing high performance biosensor for reliable detection and management of blood glucose concentration. Meanwhile, the technology advance can also facilitate the application of glucose sensor in industrial, agriculture, and environmental monitoring (Cho et al. 2008; Lee et al. 2008; Vaddiraju et al. 2010; Wang et al. 2017; Xu et al. 2004).

Currently, enzymatic glucose sensors are available commercially. The enzyme electrode was first proposed by Clark and Lyons in 1962 (Clark and Lyons 1962). Albeit their readiness, they are expensive and exhibit poor stability because of the surface poisoning by chloride and other intermediates. Therefore, nonenzymatic catalysts for glucose sensing has been widely explored. The examples include noble metal (Au (Chen et al. 2015) and Pt (Nantaphol et al. 2017)), transition metal (Ni (Zhang et al. 2017), Cu (Shi et al. 2016), and Co (Ramachandran et al. 2016)), and transition metal oxides ($NiO/Ni(OH)_2$ (Huang et al. 2017), CuO (Zhuang et al. 2008), and Co_3O_4 (Ding et al. 2010)). Among them, copper nanoparticle (Cu-NP) is a promising candidate because of its excellent conductivity, low-cost, good stability, and good catalytic activity for glucose (He et al. 2017; Yang et al. 2016).

Typically, Cu-NPs based glucose sensors are fabricated chemically or electrochemically. The chemical synthesis usually involves hydrothermal treatment, high-temperature heating, or other complicated processes, which are energy-consuming and could result in impurities that hinder the glucose sensing (Shi et al. 2016; Terzi et al. 2017; Wang et al. 2015; Yi et al. 2015). Binder or other additives are often used in the synthetic process (*eg.* polyvinyl pyrrolidone (PVP) and Nafion (Liu et al. 2014; Yi et al. 2015)), further decreasing the electron transfer of copper catalysts. These drawbacks significantly affect the linear range and the limit of detection (LOD) of the sensors. In contrast, the electrochemical synthesis provides a facile approach to produce Cu-NPs. However, the catalytic activity of the electrodeposited Cu-NPs changes dramatically across electrodes with different surface characteristics (Shi et al. 2016; Yang et al. 2016). A conductive substrate with abundant active sites for the deposition of Cu-NPs is highly desirable for the producing high-performance Cu-NPs based glucose sensors.

Meanwhile, continuous daily monitoring of blood-glucose level is critical for the effective management of diabetes. Implantable glucose biosensor has recently attracted lots of interests from both academia and industry. Currently, the glucose sensing catalyst, enzymatic or nonenzymatic, are typically immobilized on hard substrates, including glassy carbon (Liu et al. 2014; Xu et al. 2016), SiO_2 (Li et al. 2011), carbon nanotubes (Rahman et al. 2009), TiO_2 (Benvenuto et al. 2009), ZnO (Kong et al. 2009), and Au (Yan et al. 2008) etc. The lack of flexibility hinders the application of these substrates in flexible and implantable sensors. Hence,

developing a flexible conductive substrate is critical for advancing the technology.

In 2012, El-Kady *et. al*. reported a method of producing graphene by a mass-produced LightScribe DVD optical drive (El-Kady and Kaner 2013; El-Kady et al. 2012; Strong et al. 2012). This low-cost approach produces highly conductive laser-scribed graphene (LSG) with large surface area in defined patterns on a flexible substrate. Moreover, the laser-induced wrinkles and ruptures on the graphene surface serve as highly active sites for further electrochemical reactions. Here, we successfully fabricate a flexible and highly sensitive nonenzymatic glucose sensors using a flexible LSG electrode. Cu-NPs are decorated on the LSG electrode electrochemically as the glucose oxidizing catalyst. The flexible LSG/Cu-NPs glucose sensor exhibits a linear detection range from 1 μM to 4.54 mM with a low LOD of 0.35 μM. Furthermore, this nonenzymatic glucose sensor demonstrates excellent reproducibility, stability, and flexibility while showing resistance to interfering substance. The fabrication of LSG/Cu-NPs glucose sensor provide a cost-effective alternative for the large scale production flexible sensing devices.

2. Experimental

2.1. Chemicals

Natural graphite (99.95%, 1.3 μm), $CuSO_4$, glucose, lactose (LA) and sucrose are purchased from Aladdin (Shanghai, China), Sodium hydroxide (NaOH), copper sulphate ($CuSO_4$), dopamine (DA), 4-acetamidophenol (AP), sodium sulphate (Na_2SO_4) are obtained from Sinopharm Chemical Reagent Co. Ltd (Shanghai,China). Sodium chloride (NaCl), uric acid (UA), ascorbic acid (AA), d-fructose are purchased from Xilong Scientific Co. Ltd (Shanghai, China). Deionized water (18.2 MΩ cm) is used for all solution preparations. All chemicals are of analytical grade and used as received without further purification.

2.2. Fabrication of laser-scribed graphene (LSG) electrode

Graphene oxide (GO) is synthesized from natural graphite following the improved Hummers' method (Marcano et al. 2010). A 4 mg/mL GO aqueous suspension is prepared by adding 0.4 g GO powder into 100 mL water and sonicating the mixture for 20 min. Scheme 1 illustrates the procedure for fabricating an LSG electrode. First, the as-prepared GO suspension is coated evenly onto a piece of polyimide (PI) foil by the doctor blade method. The PI foil is dried under ambient condition and then pasted onto a DVD disc. A standard LightScribe DVD optical drive is adopted to print various specific patterns on the LSG loaded PI foil for 5 times. The size of LSG pad can be designed using the software Nero CoverDesigner. After the laser-printing, the PI foil is peeled off from the disc and cut into the designed shape (Fig. S1). To form electrical contact, a strip of cooper foil is connected to the edge of the LSG pad via conductive silver paint. The whole electrode is then encapsulated with silicone rubber, leaving a 3 mm × 3 mm window for electrochemical sensing. The same process can be done on other flexible substrates, such as polycarbonate (PC) or metal foil.

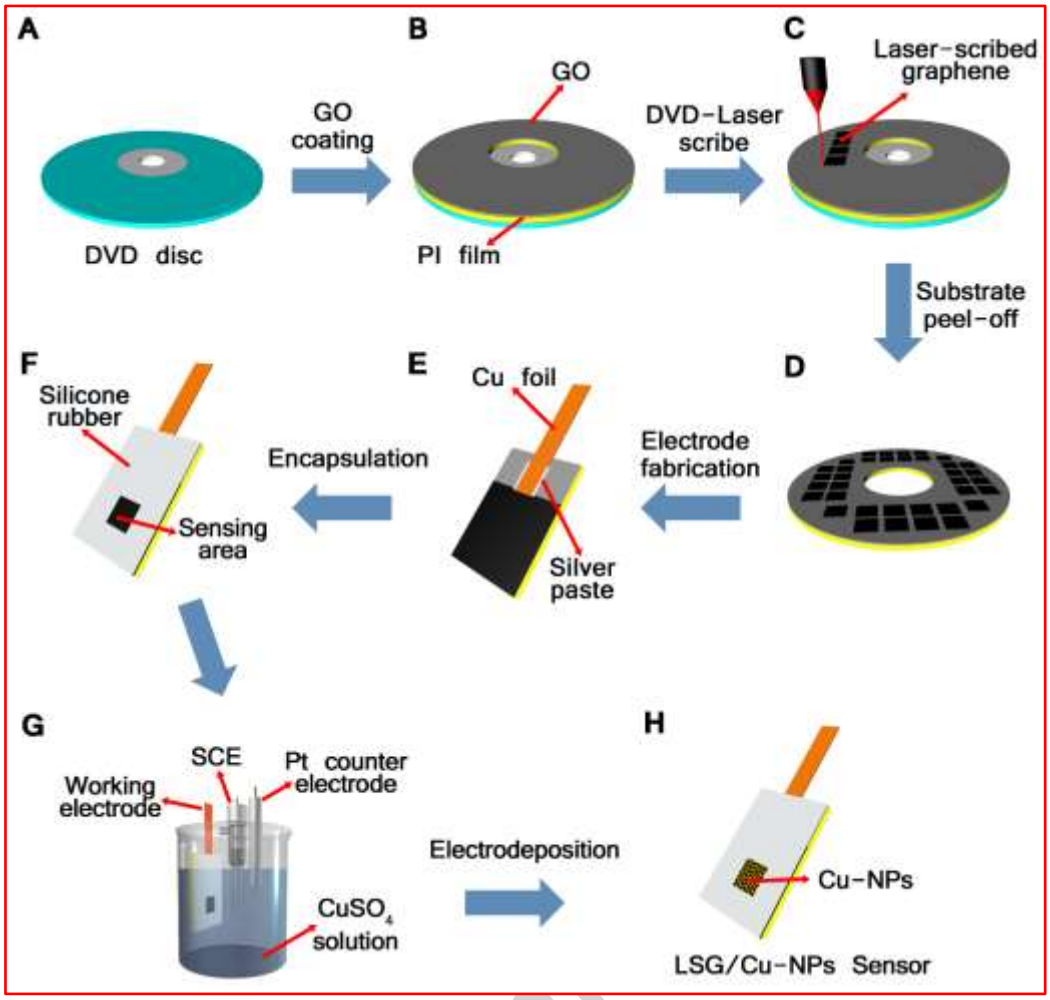

Scheme 1. Schematic illustration of the fabrication process of flexible LSG glucose sensor. (A to D) A GO film supported on PI foil is pasted on a DVD disc and a designed pattern is printed on the GO film by a mass-produced LightScribe DVD drive. The color of the reduced area on the GO film changes from brown to black (also see Fig. S1); (E) A stripe of copper foil is attached to the printed area to make electrical contact; (F) Silicone rubber is used to encapsulate the device and define the sensing window; (G) Copper nanoparticles (Cu-NPs) are electrodeposited on the LSG substrate; (H) The finished LSG/Cu-NPs sensor.

2.3 Fabrication of chemically reduced graphene oxide (CRGO) electrode

500 mg of GO is dispersed in 200 mL of DI water and sonicated for 50 min to form a 2.5 mg/ml GO solution. 5 ml of hydrazine hydrate is added into the GO solution. The mixture is stirred at 90°C for 24 h. The solid product is collected by centrifugation and dried in vacuum to obtain the chemically reduced graphene oxide (CRGO). CRGO powder is mixed with styrene-butadiene rubber (SBR) binder in a weight ratio of 9:1 in N-Methyl pyrrolidone (NMP) to create a homogeneous paste. The paste is coated onto the PI foil and dried in vacuum. The CRGO coated PI foil is cut to the designed shape and processed into the encapsulated sensor following the same procedure in section 2.2.

2.4 Electrochemically decoration of copper nanoparticles (Cu-NPs) on the sensing area

The Cu-NPs are decorated on the sensing area via potentiostatic deposition. The deposition is

done using a three-electrode setup with the encapsulated LSG electrode as the working electrode, saturated calomel electrode (SCE) as the reference electrode, and platinum wire as the counter electrode. A solution (100 mL) containing 0.1 M Na_2SO_4 and 0.01 M $CuSO_4$ is used as the electrolyte and copper source. A constant potential of -0.4 V (vs. SCE) is applied for 480 s, resulting in the Cu-NPs decorated LSG sensor (LSG/Cu-NPs). The electrodeposition parameters are optimized experimentally (see Supplementary Information and Fig. S2-S3 for more details). Subsequently, the LSG/Cu-NPs sensor is washed with DI water and dried in air. By replacing the LSG working electrode, Cu-NPs are also decorated onto the copper foil and the CRGO electrode using the same method, resulting in the CF/Cu-NPs and CRGO/Cu-NPs sensors.

2.5. Materials Characterization

Microstructure, morphology, and composition of the as-obtained LSG, LSG/Cu-NPs, CRGO/Cu-NPs, and CF/Cu-NPs sensors are characterized by scanning electron microscopy (SEM, Hitachi SU8010). X-ray diffraction (XRD) patterns are collected on a Bruker D8 ADVANCE diffractometer equipped with Cu Kα radiation. Raman spectra are recorded on a Lab RAMHR800 (using a 532 nm laser as excitation source). X-ray photoelectron spectroscopy (XPS) measurements are done on a Thermo Scientific ESCALAB 250Xi.

2.6. Electrochemical Characterization

All electrochemical characterizations are performed on an electrochemical workstation (Wavedrive10, PINE) in a standard three-electrode cell. The LSG/Cu-NPs, LSG, CRGO/Cu-NPs, or CF/Cu-NPs sensor is used as the working electrode, respectively, with a platinum counter electrode and SCE reference electrode. All the measurements are carried out in 0.1 M NaOH solution at room temperature (the effect of NaOH concentration on glucose oxidation is discussed in the Supplementary Information and Fig. S4). Amperometric measurements are performed by consecutive addition of known amount of glucose into the NaOH solution under constant stirring. The catalytic performance of the sensors is evaluated with cyclic voltammetry (CV) and chronoamperometry.

3. Results and discussions

3.1. Characterization of surface morphology and composition

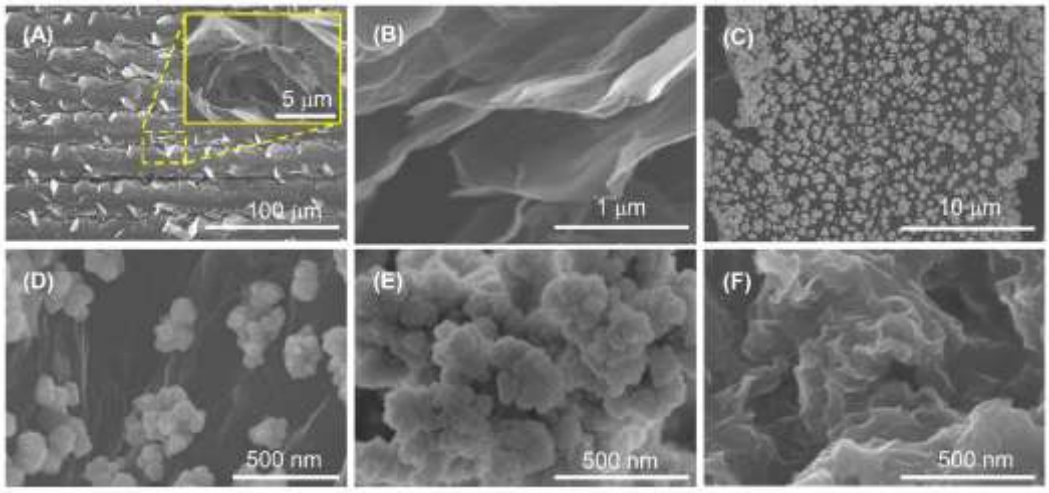

Fig. 1. SEM images of the surface of (A) and (B) the as-prepared LSG, (C) and (D) LSG/Cu−NPs, (E) CF/Cu-NPs, and (F) CRGO/Cu-NPs.

The surface morphology of the LSG, LSG/Cu-NPs, CF/Cu-NPs, and CRGO/Cu-NPs electrode is characterized by SEM (Fig. 1 and Fig. S5). We observe significant rupturing on the LSG surface (Fig. 1A). These ruptures, introduced by the laser scribing during GO reduction, improve the surface area significantly (inset of Fig. 1A) and increase active sites for the catalyst deposition. The exposed graphene sheets at the ruptured area appear almost transparent, showing its few-layer characteristics (Fig. 1B). The SEM image of the LSG/Cu-NPs sensor (Fig. 1C and 1D) reveals that the Cu-NPs (about 50 nm) distribute uniformly on the LSG surface. The uniformly distributed Cu-NPs can also be observed from the EDS mapping (Fig. S5). It is worth noticing that more Cu-NPs are decorated at the ruptured region of LSG, indicating that the defects likely serve as nucleation site for Cu-NPs. This unique microstructure provides abundant catalytic sites for the oxidation of glucose. From the cross-sectional SEM image (Fig. S6), we can see that the graphene on the LSG/Cu-NPs sensor are divided into two parts, with the top 35-μm portion being reduced and providing large sensing surface. The Cu-NPs is deposited on the outermost layer of the 35-μm reduced graphene. Meanwhile, evenly distributed Cu-NPs are observed on CF/Cu-NPs (Fig. S7). However, because of the insufficient nucleation site on the smooth CF surface, the Cu-NPs form micron-size aggregates (Fig. 1E). The limited electrode surface and the Cu-NPs agglomeration both decrease the active sensing sites and could lead to poor performance. Finally, on the CRGO/Cu-NPs, few Cu-NPs can be observed (Fig. 1F and Fig. S7B), indicating insufficient catalyst deposition.

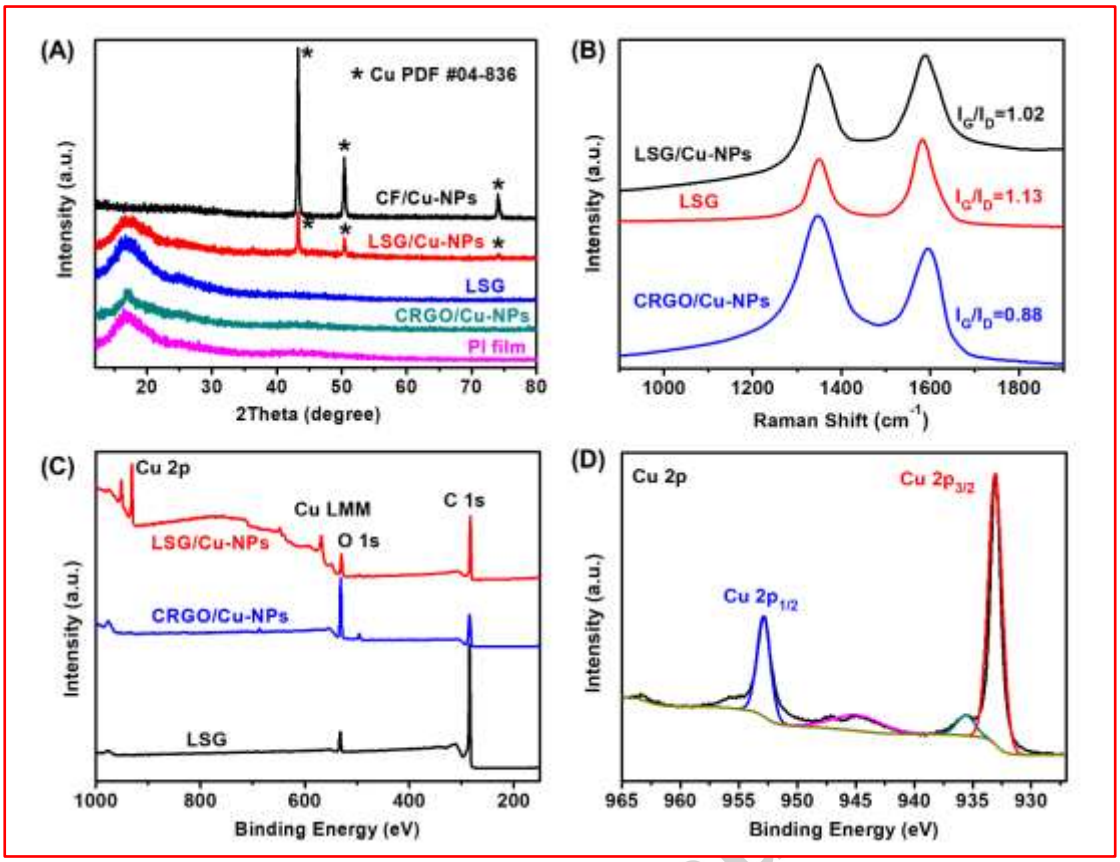

Fig. 2. (A) XRD spectra of different samples; (B) Raman spectra of LSG/Cu-NPs, LSG, and CRGO/Cu-NPs; (C) XPS spectra of LSG/Cu-NPs, CRGO/Cu-NPs, and LSG. (D) High-resolution Cu 2p XPS spectrum of LSG/Cu-NPs.

Fig. 2A shows the XRD patterns of the LSG, LSG/Cu-NPs, CF/Cu-NPs, CRGO/Cu-NPs, and PI foil. For the LSG/Cu-NPs, there are three strong diffraction peaks at 43.3°, 50.4° and 74.1°, corresponding to the (111), (200), and (220) lattice planes of Cu (JCPDS: No. 04-836). This confirms that the Cu-NPs are successfully deposited onto the LSG. No obvious diffractions are observed for the CRGO/Cu-NPs sensor, consistent with its SEM image . For LSG/Cu-NPs, LSG, and CRGO/Cu-NPs, a broad hump near 25° is observed, which can be attributed to the reduced graphene. In the Raman spectrum (Fig. 2B), two characteristic bands (D and G) of graphitized carbon (1350 and 1590 cm^{-1}) can be observed, with I_G/I_D value equals to 1.02, 1.13, and 0.88 for LSG/Cu-NPs, LSG, and CRGO/Cu-NPs, respectively. Since higher I_G/I_D indicates higher degree of reduction (Muradyan et al. 2013), this proves that the DVD-laser reduces graphene more thoroughly than the chemical reduction method. Incomplete reduction in CRGO inevitably leads to low conductivity, which hinders the Cu-NPs growth.

The XPS survey spectra (in Fig. 2C) confirms the presence of Cu and O on the surface of the LSG/Cu-NPs. No noticeable copper signal is observed on the CRGO/Cu-NPs electrode, consistent with the SEM and XRD observations. The O 1s peak is the most pronounced for the CRGO/Cu-NPs electrode, indicating its low degree of graphene reduction. The high resolution Cu 2p XPS spectrum (Fig. 2D) shows that only zero-valent Cu presents on LSG/Cu-NPs (with a 19.8 eV spin-energy separation between the Cu $2p_{3/2}$ and Cu $2p_{1/2}$ peaks) (Amri et al. 2013; Weng et al.

2016), which is also confirmed according to the Cu Auger region (Fig. S8A). Meanwhile, the C 1s spectrum (Fig. S8B) of LSG/Cu-NPs can be fitted into three peaks at 284.8, 285.8, and 288.5 eV, corresponding to the C=C/C-C, C-O, and C=O bonds, respectively. The weak signal from O 1s spectrum of LSG/Cu-NPs (Fig. S8C) comes from the residual oxygen groups on graphene surface.

3.2 Electrocatalytic oxidation of glucose on the LSG/Cu-NPs sensor

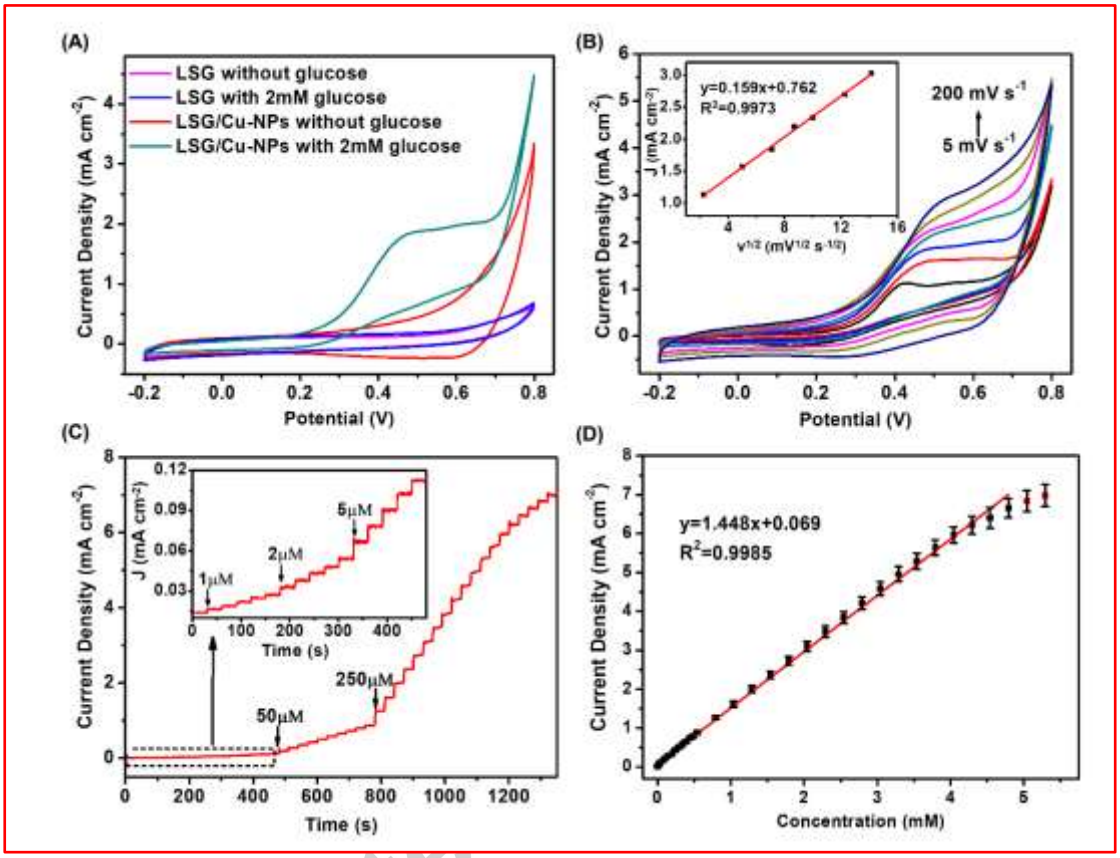

Fig. 3. (A) Cyclic voltammograms of the LSG and LSG/Cu-NPs electrode in the absence and presence of 2.0 mM glucose in 0.1 M NaOH. Scan rate: 50 mV s^{-1}; (B) Cyclic voltammograms of LSG/Cu-NPs under various scan rates, including 5, 25, 50, 75, 100, 150, and 200 mV s^{-1}, respectively. Inset: plot of peak current vs. the square root of scan rate; (C) Typical amperometric response of the LSG/Cu-NPs sensor at 0.6 V to successive addition of glucose in 0.1 M NaOH; (D) The corresponding calibration curve of the LSG/Cu-NPs sensor with the linear fitting result.

The electrocatalytic properties of the LSG/Cu-NPs, CF/Cu-NPs, CRGO/Cu-NPs, and LSG sensors are investigated by cyclic voltammetry (Fig. 3A and Fig. S9). In the absence of glucose, no oxidation peaks are observed for all electrodes. With the addition of 2 mM glucose, the LSG electrode shows little responses; the LSG/Cu-NPs electrode, on the other hand, exhibits significant oxidation current starting from 0.25 V vs. SCE and reaches a plateau between 0.45 V and 0.7 V vs. SCE. The plateau corresponds to the continuous glucose oxidation (Fig. 3A). Compared with the CF/Cu-NPs electrode (Fig. S9), the LSG/Cu-NPs electrode exhibits much higher sensing current (Fig. 3A). The enhanced electrocatalytic performance can be attributed to the large accessible surface and the uniformly distributed Cu-NPs. The synergistic effect significantly enhances the

electrochemical oxidation of glucose on LSG/Cu-NPs.

CV study of various glucose concentrations (0-3 mM) in 0.1 M NaOH is also carried out under a 50 mV s^{-1} scan rate. From Fig. S10, we observe that the oxidation current on LSG/Cu-NPs increases with glucose concentration. To study the electrochemical kinetics of this catalytic process, we measure the CV curves under different scan rates (5 to 200 mV s^{-1}) in 2 mM glucose solution (Fig. 3B). The current increases with increasing scan-rate while the oxidation potential shifted from 0.45 V to 0.50 V (vs. SCE). The relation (Fig. 3B inset) between the current and the scan rate can be described by equation [1]:

$$J = 0.159v^{1/2} + 0.762,\ (R^2 = 0.9973) \quad [1]$$

where J (unit: mA cm^{-2}) is the peak current density and ν (unit: mV s^{-1}) is the scan rate of the applied potential. The linear relationship between J and $\nu^{1/2}$ indicates that the catalytic process is diffusion-controlled (Shi et al. 2016).

3.3. Amperometric response of the LSG/Cu-NPs glucose biosensor

As we know, the applied potential strongly affects the amperometric response of a biosensor. Prior to the test, we have carefully determined that 0.6 V (vs. SCE) is the optimum potential for sensing glucose with LSG/Cu-NPs (Fig. S11). Fig. 3C shows the amperometric response of LSG/Cu-NPs under constant addition of glucose. After introducing the glucose, the current increases immediately and maintains stable. It is worth mentioning that even a tiny increase in glucose concentrations (by 1 μM) creates noticeable response current (Fig. 3C inset). The linear detection range of LSG/Cu-NPs for glucose spans from 1 μm to 4.54 mM (Fig. 3D). Its amperometric response can be fitted by equation [2]:

$$J = 0.069 + 1.448C,\ (R^2 = 0.9986) \quad [2]$$

where J (unit: mA cm^{-2}) and C (unit: mM) stand for the current density and the glucose concentration, respectively. Based on the equation, the LSG/Cu-NPs sensor demonstrates a high sensitivity of 1.518 mA mM^{-1} cm^{-2}. The limit of detection is as low as 0.35 μM according to equation [3]:

$$\mathrm{LOD} = \frac{3 \times \mathrm{N}}{\mathrm{s}} \quad [3]$$

where N is the standard deviation of the LSG/Cu-NPs sensor's current output in 0.1 M NaOH solution and s is the slope of the calibration curve (Naik et al. 2017).

To apply the LSG/Cu-NPs sensor to a wider detection range for practical situations, Langmuir isothermal theory can be used to fit the calibration curve because the electrochemical oxidation of glucose is a surface catalytic reaction (Ding et al. 2010). As shown in Fig. S12, the corresponding equation can be expressed as [4]:

$$J = 20.347 \times C/(9.451 + C),\ (R^2 = 0.9993) \quad [4]$$

where J (unit: mA cm^{-2}) and C (unit: mM) stand for the current density and the glucose concentration, respectively. This equation covers a broader glucose concentration range from 0.1 to 14 mM.

It is important to notice that although Cu-NPs are originally deposited, the catalytically active species likely contain Cu of higher oxidation states because surface oxides are expected to form on copper at 0.6 V vs. SCE in 0.1 M NaOH solution (Hepel 1999; Hepel and Stobiecka 2007). Currently, the most accepted mechanism for glucose oxidization on copper in alkaline solution involves the interaction between glucose and Cu(I) and Cu(II) (Marioli and Kuwana 1992; Wang et al. 2012; Zhou et al. 2014). The potential formation of Cu(III) at high potential might also play an important role during catalytic oxidation (Wels and Johnson 1990). After the glucose sensing, we collect the XRD pattern of the LSG/Cu-NPs and find the formation of Cu_2O on the sensing area (Fig. S13). With Cu-metal signal remaining in the XRD pattern (Fig. S13), Cu_2O likely forms on the surface of Cu-NPs and serve as the true catalyst during glucose oxidation. In addition, XPS spectrum also confirms the formation of copper oxide on LSG/Cu-NPs after glucose sensing (Fig. S14).

3.4 Sensing performance, reproducibility, stability, and flexibility of LSG/Cu-NPs glucose sensor

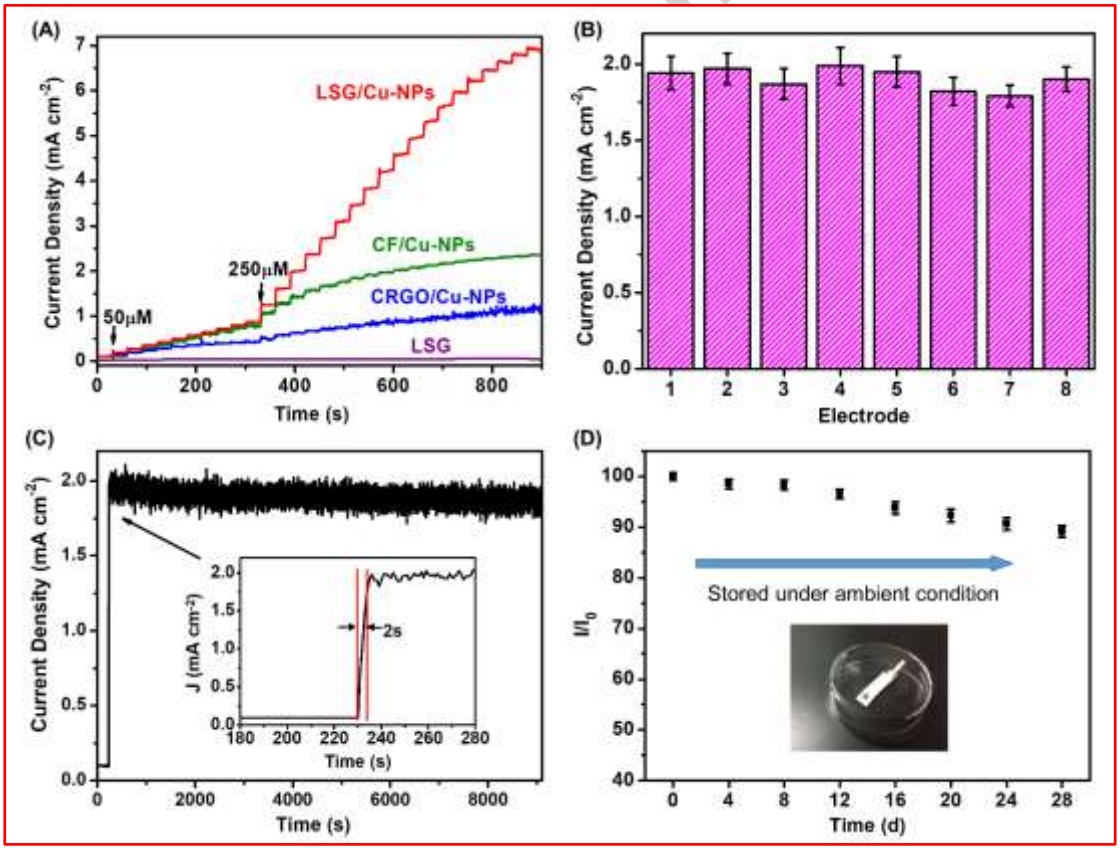

Fig. 4. (A) Amperometric response of LSG/Cu-NPs, CF/Cu-NPs, CRGO/Cu-NPs and LSG electrodes with successive additions of glucose to 0.1 M NaOH; (B) Amperometric responses of eight different LSG/Cu-NPs

sensors to 1 mM glucose in 0.1 M NaOH; (C) Amperometric response of the LSG/Cu-NPs sensor to 1 mM glucose in 0.1 M NaOH over 9000 s (Insert: The response time for the sensor to achieve steady current output); (D) Amperometric response of the LSG/Cu-NPs sensor to 1 mM glucose in 0.1 M NaOH after stored at ambient conditions for different period. The applied potential is 0.6 V vs. SCE in all measurements.

The LSG/Cu-NPs sensor exhibits superior amperometric response comparing to the LSG, CF/Cu-NPs, and CRGO/Cu-NPs sensors (Fig. 4A). This is as expected. For the LSG sensor, the current level maintains almost constant with the addition of glucose because of the lack of electrocatalyst. For CF/Cu-NPs, the linear detection range terminates at <1 mM while significant attenuation is observed on the current response level. This is caused by the limited surface area and hence the limited catalytic sites on CF/Cu-NPs, making it incapable of handling high glucose concentration. Finally, the CRGO/Cu-NPs sensor exhibits poor amperometric response with fast decaying response level. Although CRGO has larger surface area, the insufficient Cu-NPs deposition renders its poor catalytic activity. To demonstrate the superior performance of LSG/Cu-NPs glucose sensor, we compare it with recently reported glucose sensors based on copper or other catalysts. As shown in Table S1, the LSG/Cu-NPs glucose sensor exhibits relatively high sensitivity and low LOD among the listed sensors, demonstrating excellent overall performance.

We investigate the reproducibility of our fabrication process by testing eight different LSG/Cu-NPs sensors under the same operating conditions. Three measurements are done in 0.1 M NaOH with 1 mM glucose on each sensor (Fig. 4B). The resulted relative standard deviation value (RSD %) of the amperometric response is 3.79%, indicating the good reproducibility of our process.

In Fig. 4C, we observe that the LSG/Cu-NPs sensor maintains 95% of its current level after injecting 1 mM glucose into the 0.1 M NaOH solution for 9000 seconds, which demonstrates its excellent current stability. In addition, after adding the glucose, the LSG/Cu-NPs sensor quickly reaches a steady current level in about 2 s. The rapid response and the excellent stability are both critical for practical applications. The long-term storage stability of the LSG/Cu-NPs sensor is also examined by measuring the amperometric response of a LSG/Cu-NPs sensor to 1 mM glucose once every 4 days over a period of 4 weeks. The sensor is stored under ambient condition without special protection during the experiment period. After 4 weeks, the current response remains at about 90% of its initial value (Fig. 4D), demonstrating the robustness of the device.

To test the flexing stability, a LSG/Cu-NPs sensor is bent against a 4-mm diameter rod for multiple times. No significant change in current response are observed after bending the sensor for 30 times (Fig. S15). Notably, the sensor maintains 83.9% of its initial current response after bending for 180 times. The calibration curves of the LSG/Cu-NPs sensor after different bending cycles are shown in Fig. 5A. We can see that the sensor exhibits linear current response over a concentration range from 0 to 5 mM and maintains both its sensitivity and the correlation coefficient (Fig. 5B). These results demonstrated the extraordinary flexing stability of the LSG/Cu-NPs sensors.

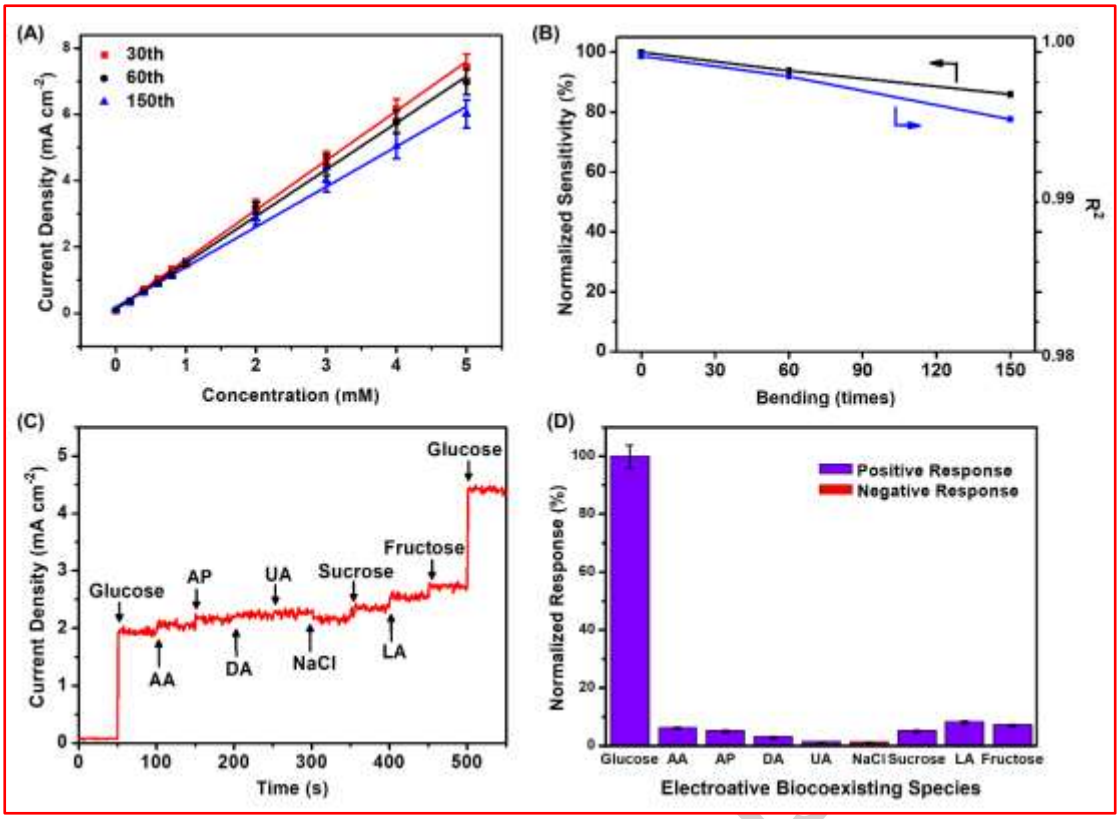

Fig. 5. (A) Calibration curves of the LSG/Cu-NPs sensor after bending the device around a 4-mm diameter rod for different times; (B) The change of normalized sensitivity and the R^2 factor of the LSG/Cu-NPs sensor over 150 bending times; (C) Interference test of the LSG/Cu-NPs sensor in 0.1 M NaOH solution containing the 1 mM of glucose and the 0.1 mM of interfering species. (D) The percentage current signals compared of the interfering species to glucose. The applied potential is 0.6 V vs. SCE in all measurements.

3.5 Anti-interference property and simulative serum sample analysis

In human blood, there are a lot of oxidizable species that can interfere with glucose detection. Examples include ascorbic acid (AA), 4-acetamidophenol (AP), dopamine (DA), uric acid (UA), and various carbohydrate compounds (*e.g.* sucrose, fructose, and lactose). A glucose biosensor needs to precisely detect the glucose level under the presence of these compounds. The typically level of glucose in human blood is 3.0–8.0 mM, which is at least thirty times higher than the interfering substances (below 0.1 mM) (Zhuang et al., 2008). Therefore, the anti-interference property is tested by successive injection of 1 mM of glucose and 100 μM of interfering species into 0.1 M NaOH solution (Fig. 5C). In Fig. 5D, we observe that the addition of interfering species produce negligible current response ratio from 1.45% (uric acid) to 8.37% (LA) relative to glucose. Meanwhile, the current response ratio of chloride is 1.27% relative to glucose.

Meanwhile, despite the complexity of human serum, there are only a few electrochemically oxidizable species (*e.g.* uric acid (UA), ascorbic acid (AA), and 4-acetamidophenol (AP)) with electron transfer rates higher than that of glucose. Their high electron transfer rate could result in significant interference with glucose detection even at a low concentration (Nantaphol et al. 2017). Thus, we perform test in three simulant serums containing 20 μM UA, 100 μM AA, and 100 μM

AP, respectively. The amperometric response is measured with the LSG/Cu-NPs sensor after injecting different amount of glucose into the simulant serums. The glucose concentration is determined based on the calibration curve of LSG/Cu-NPs. In all samples, the ratio between the measured value and the actual value is in the range of 96.8–101.6% with RSD% value ranging from 1.8 to 5.1% (Table S2). Therefore, the LSG/Cu-NPs sensor experiences little interference from these fast-electron-transferring species during glucose detection, which demonstrates its great potential for practical application.

4. Conclusions

We have successfully fabricated a high-performance flexible LSG/Cu-NPs glucose sensor by exploiting the DVD-laser scribed graphene substrate. This novel flexible substrate, with abundant active sites and high electron conductivity, is ideal for the electrodeposition of Cu-NPs catalyst. The LSG/Cu-NPs glucose sensor demonstrates a wide linear glucose detection range from 1 μM to 4.54 mM with high sensitivity (1.518 mA mM^{-1} cm^{-2}) and low limit of detection (0.35 μM). Moreover, it also exhibits excellent flexing stability and anti-interference property. The LSG substrate can serve as a versatile and flexible electrode for the electrodeposition of catalysts, which can enable the detection of various organic or inorganic compounds. This points to a promising direction for further developing other high performance flexible biosensors and bioelectronics beyond LSG/Cu-NPs glucose sensor.

Acknowledgments

We thank the financial support from the National Natural Science Foundation of China (Grant No. 51602310) and the Fujian Provincial Department of Science and Technology (Grant No. 2018H01010111, 2018H01010112, 2016H0047, 2016T3011, 2016T3027, 2016T3031, 2016T3022, and 2018T3010).

References

Amri, A., Duan, X., Yin, C.-Y., Jiang, Z.-T., Rahman, M.M., Pryor, T., 2013. Solar absorptance of copper–cobalt oxide thin film coatings with nano-size, grain-like morphology: Optimization and synchrotron radiation XPS studies. Applied Surface Science 275, 127-135.

Benvenuto, P., Kafi, A.K.M., Chen, A., 2009. High performance glucose biosensor based on the immobilization of glucose oxidase onto modified titania nanotube arrays. Journal of Electroanalytical Chemistry 627(1-2), 76-81.

Chen, A., Ding, Y., Yang, Z., Yang, S., 2015. Constructing heterostructure on highly roughened caterpillar-like gold nanotubes with cuprous oxide grains for ultrasensitive and stable nonenzymatic glucose sensor. Biosensors & bioelectronics 74, 967-973.

Cho, J.I., Ryoo, N., Eom, J.S., Lee, D.W., Kim, H.B., Jeong, S.W., Lee, Y.H., Kwon, Y.K., Cho, M.H., Bhoo, S.H., Hahn, T.R., Park, Y.I., Hwang, I., Sheen, J., Jeon, J.S., 2008. Role of the Rice Hexokinases OsHXK5 and OsHXK6 as Glucose Sensors. Plant Physiology 149(2), 745-759.

Clark, L.C., Lyons, C., 1962. ELECTRODE SYSTEMS FOR CONTINUOUS MONITORING IN CARDIOVASCULAR SURGERY. Annals of the New York Academy of Sciences 102(1), 29-45.

Ding, Y., Wang, Y., Su, L., Bellagamba, M., Zhang, H., Lei, Y., 2010. Electrospun Co3O4 nanofibers for

sensitive and selective glucose detection. Biosensors & bioelectronics 26(2), 5428.

El-Kady, M.F., Kaner, R.B., 2013. Scalable fabrication of high-power graphene micro-supercapacitors for flexible and on-chip energy storage. Nature communications 4, 1475.

El-Kady, M.F., Strong, V., Dubin, S., Kaner, R.B., 2012. Laser scribing of high-performance and flexible graphene-based electrochemical capacitors. Science 335(6074), 1326-1330.

He, Y., Wei, G., Lin, J., Sun, M., Li, Z., 2017. Cu and Ni Nanoparticles Deposited on ITO Electrode for Nonenzymatic Electrochemical Carbohydrates Sensor Applications. Electroanalysis 29(4), 965-974.

Hepel, M., 1999. Electrode-Solution Interface Studied with Electrochemical Quartz Crystal Nanobalance. In: Wieckowski, A. (Ed.), Interfacial Electrochemistry. Theory, Experiment, and Applications, pp. 599-631. M. Dekker, New York.

Hepel, M., Stobiecka, M., 2007. Interactions of adsorbed albumin with underpotentially deposited copper on gold piezoelectrodes. Bioelectrochemistry 70(1), 155-164.

Huang, W., Ge, L., Chen, Y., Lai, X., Peng, J., Tu, J., Cao, Y., Li, X., 2017. Ni(OH) 2 /NiO nanosheet with opulent active sites for high-performance glucose biosensor. Sensors and Actuators B: Chemical 248, 169-177.

Kong, T., Chen, Y., Ye, Y., Zhang, K., Wang, Z., Wang, X., 2009. An amperometric glucose biosensor based on the immobilization of glucose oxidase on the ZnO nanotubes. Sensors and Actuators B: Chemical 138(1), 344-350.

Lee, S.R., Lee, Y.T., Sawada, K., Takao, H., Ishida, M., 2008. Development of a disposable glucose biosensor using electroless-plated Au/Ni/copper low electrical resistance electrodes. Biosensors & bioelectronics 24(3), 410-414.

Li, H., He, J., Zhao, Y., Wu, D., Cai, Y., Wei, Q., Yang, M., 2011. Immobilization of glucose oxidase and platinum on mesoporous silica nanoparticles for the fabrication of glucose biosensor. Electrochimica Acta 56(7), 2960-2965.

Liu, L., Chen, Y., Lv, H., Wang, G., Hu, X., Wang, C., 2014. Construction of a non-enzymatic glucose sensor based on copper nanoparticles/poly(o-phenylenediamine) nanocomposites. Journal of Solid State Electrochemistry 19(3), 731-738.

Marcano, D.C., Kosynkin, D.V., Berlin, J.M., Sinitskii, A., Sun, Z., Slesarev, A., Alemany, L.B., Lu, W., Tour, J.M., 2010. Improved Synthesis of Graphene Oxide. ACS Nano 4(8), 4806-4814.

Marioli, J.M., Kuwana, T., 1992. Electrochemical characterization of carbohydrate oxidation at copper electrodes. Electrochimica Acta 37(7), 1187-1197.

Muradyan, V.E., Arbuzov, A.A., Sokolov, E.A., Babenko, S.D., Bondarenko, G.V., 2013. The effect of addition of functionalized graphene oxide on the dielectric properties of epoxy composite. Technical Physics Letters 39(9), 798-800.

Naik, K.K., Gangan, A., Chakraborty, B., Nayak, S.K., Rout, C.S., 2017. Enhanced Nonenzymatic Glucose-Sensing Properties of Electrodeposited NiCo2O4-Pd Nanosheets: Experimental and DFT Investigations. ACS applied materials & interfaces 9(28), 23894-23903.

Nantaphol, S., Watanabe, T., Nomura, N., Siangproh, W., Chailapakul, O., Einaga, Y., 2017. Bimetallic Pt-Au nanocatalysts electrochemically deposited on boron-doped diamond electrodes for nonenzymatic glucose detection. Biosensors & bioelectronics 98, 76-82.

Rahman, M.M., Umar, A., Sawada, K., 2009. Development of amperometric glucose biosensor based on glucose oxidase co-immobilized with multi-walled carbon nanotubes at low potential. Sensors and Actuators B: Chemical 137(1), 327-333.

Ramachandran, K., Raj Kumar, T., Babu, K.J., Gnana Kumar, G., 2016. Ni-Co bimetal nanowires filled

multiwalled carbon nanotubes for the highly sensitive and selective non-enzymatic glucose sensor applications. Scientific reports 6, 36583.

Shi, L., Zhu, X., Liu, T., Zhao, H., Lan, M., 2016. Encapsulating Cu nanoparticles into metal-organic frameworks for nonenzymatic glucose sensing. Sensors and Actuators B: Chemical 227, 583-590.

Shi, Y., Hu, F.B., 2014. The global implications of diabetes and cancer. The Lancet 383(9933), 1947-1948.

Strong, V., Dubin, S., El-Kady, M.F., Lech, A., Wang, Y., Weiller, B.H., Kaner, R.B., 2012. Patterning and Electronic Tuning of Laser Scribed Graphene for Flexible All-Carbon Devices. ACS Nano 6(2), 1395-1403.

Terzi, F., Zanfrognini, B., Ruggeri, S., Dossi, N., Casagrande, G.M., Piccin, E., 2017. Amperometric paper sensor based on Cu nanoparticles for the determination of carbohydrates. Sensors and Actuators B: Chemical 245, 352-358.

Vaddiraju, S., Tomazos, I., Burgess, D.J., Jain, F.C., Papadimitrakopoulos, F., 2010. Emerging synergy between nanotechnology and implantable biosensors: a review. Biosensors & bioelectronics 25(7), 1553-1565.

Wang, A.-J., Feng, J.-J., Li, Z.-H., Liao, Q.-C., Wang, Z.-Z., Chen, J.-R., 2012. Solvothermal synthesis of Cu/Cu2O hollow microspheres for non-enzymatic amperometric glucose sensing. CrystEngComm 14(4), 1289-1295.

Wang, J., 2008. Electrochemical Glucose Biosensors. Chemical Reviews 108(2), 814-825.

Wang, Q., Wang, Q., Li, M., Szunerits, S., Boukherroub, R., 2015. Preparation of reduced graphene oxide/Cu nanoparticle composites through electrophoretic deposition: application for nonenzymatic glucose sensing. RSC Adv. 5(21), 15861-15869.

Wang, Y.H., Huang, K.J., Wu, X., 2017. Recent advances in transition-metal dichalcogenides based electrochemical biosensors: A review. Biosensors & bioelectronics 97, 305-316.

Wels, B., Johnson, D.C., 1990. Electrocatalysis of Anodic Oxygen Transfer Reactions: Oxidation of Cyanide at Electrodeposited Copper Oxide Electrodes in Alkaline Media. Journal of The Electrochemical Society 137(9), 2785-2791.

Weng, Z., Jiang, J., Wu, Y., Wu, Z., Guo, X., Materna, K.L., Liu, W., Batista, V.S., Brudvig, G.W., Wang, H., 2016. Electrochemical CO2 Reduction to Hydrocarbons on a Heterogeneous Molecular Cu Catalyst in Aqueous Solution. Journal of the American Chemical Society 138(26), 8076-8079.

Xu, J., Cao, X., Xia, J., Gong, S., Wang, Z., Lu, L., 2016. Phosphomolybdic acid functionalized graphene loading copper nanoparticles modified electrodes for non-enzymatic electrochemical sensing of glucose. Analytica chimica acta 934, 44-51.

Xu, Y., Sun, J., Mathew, G., Jeevarajan, A.S., Anderson, M.M., 2004. Continuous glucose monitoring and control in a rotating wall perfused bioreactor. Biotechnology and Bioengineering 87(4), 473-477.

Yan, Y.-M., Tel-Vered, R., Yehezkeli, O., Cheglakov, Z., Willner, I., 2008. Biocatalytic Growth of Au Nanoparticles Immobilized on Glucose Oxidase Enhances the Ferrocene-Mediated Bioelectrocatalytic Oxidation of Glucose. Advanced Materials 20(12), 2365-2370.

Yang, T., Xu, J., Lu, L., Zhu, X., Gao, Y., Xing, H., Yu, Y., Ding, W., Liu, Z., 2016. Copper nanoparticle/graphene oxide/single wall carbon nanotube hybrid materials as electrochemical sensing platform for nonenzymatic glucose detection. Journal of Electroanalytical Chemistry 761, 118-124.

Yi, W., Liu, J., Chen, H., Gao, Y., Li, H., 2015. Copper/nickel nanoparticle decorated carbon nanotubes for nonenzymatic glucose biosensor. Journal of Solid State Electrochemistry 19(5), 1511-1521.

Zhang, L., Ding, Y., Li, R., Ye, C., Zhao, G., Wang, Y., 2017. Ni-Based metal–organic framework derived

Ni@C nanosheets on a Ni foam substrate as a supersensitive non-enzymatic glucose sensor. J. Mater. Chem. B 5(28), 5549-5555.

Zhou, D.-L., Feng, J.-J., Cai, L.-Y., Fang, Q.-X., Chen, J.-R., Wang, A.-J., 2014. Facile synthesis of monodisperse porous Cu2O nanospheres on reduced graphene oxide for non-enzymatic amperometric glucose sensing. Electrochimica Acta 115, 103-108.

Zhuang, Z., Su, X., Yuan, H., Sun, Q., Xiao, D., Choi, M.M., 2008. An improved sensitivity non-enzymatic glucose sensor based on a CuO nanowire modified Cu electrode. The Analyst 133(1), 126-132.

Graphical abstract

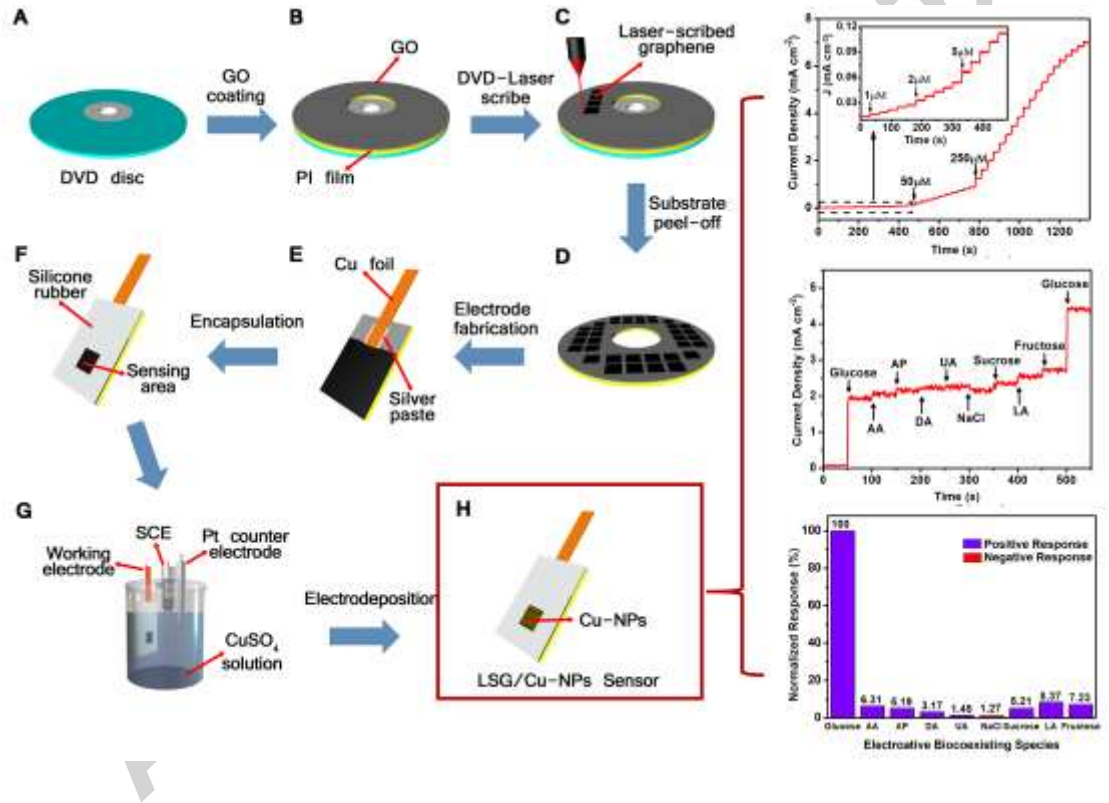

Highlights:

- A flexible and highly sensitive LSG/Cu-NPs glucose sensor is successfully fabricated;
- Cu nanoparticle catalysts are electrodeposited on a laser-scribed-graphene substrate produced by a DVD drive;
- The LSG/Cu-NPs sensor demonstrates a linear glucose detection range from 1 μM to 4.54 mM;
- The LSG/Cu-NPs sensor exhibits high sensitivity (1.518 mA mM^{-1} cm^{-2}) and low limit of detection (0.35 μM);
- Excellent flexing stability and interfering resistance are demonstrated by the LSG/Cu-NPs sensor.